

# Two-Photon-Exchange effects in $ep \rightarrow en\pi^+$ and their corrections to separated cross sections $\sigma_{L,T,LT,TT}$ at small $-t$

Hui-Yun Cao, Hai-Qing Zhou \*

School of Physics, Southeast University, NanJing 211189, China

(Dated: October 15, 2019)

In this work, the two-photon-exchange (TPE) effects in  $ep \rightarrow en\pi^+$  at small  $-t$  are discussed within a hadronic model. The TPE contributions to the amplitude and the unpolarized differential cross section are both estimated and we find that the TPE corrections to the unpolarized differential cross section are about  $-4\% \sim -15\%$  at  $Q^2 = 1\text{GeV}^2 \sim 1.6\text{GeV}^2$ . After considering the TPE corrections to the experimental data sets of unpolarized differential cross section, we analyse the TPE corrections to the separated cross sections  $\sigma_{L,T,LT,TT}$ . We find that the TPE corrections (at  $Q^2 = 1\text{GeV}^2 \sim 1.6\text{GeV}^2$ ) to  $\sigma_L$  are about  $-10\% \sim -20\%$ , to  $\sigma_T$  are about  $20\%$  and to  $\sigma_{LT,TT}$  are much larger. By these analysis, we conclude that the TPE contributions in  $ep \rightarrow en\pi^+$  at small  $-t$  are important to extract the separated cross sections  $\sigma_{L,T,LT,TT}$  and the electromagnetic magnetic form factor of  $\pi^+$  in the experimental analysis.

## I. INTRODUCTION

In the last two decades, the two-photon-exchange (TPE) effects in  $ep \rightarrow ep$  have abstracted many interesting things due to their importance in the extraction of the electromagnetic (EM) form factors of proton. Many model dependent methods have been used to estimate the TPE contributions in  $ep \rightarrow ep$  such as the hadronic model [1], GPD method [2], pQCD calculation [3], dispersion relation approach [4], SCEF method [5] and phenomenological parametrization [6]. Due to the important contributions of the TPE corrections in  $ep \rightarrow ep$ , similar TPE corrections in  $e^+e^- \rightarrow p\bar{p}$  [7],  $e\pi \rightarrow e\pi$  [8],  $\mu p \rightarrow \mu p$

---

\* E-mail: zhouhq@seu.edu.cn

[9], and  $ep \rightarrow e\Delta \rightarrow ep\pi^0$  [10] are studied aimed at the precise extraction of the EM form factor of proton in the time-like region, EM form factor of pion in the space-like region, and EM transition form factors of  $\gamma^*N\Delta$  in the space-like region from the experimental data.

Experimentally, the extraction of the EM form factor of pion via  $e\pi \rightarrow e\pi$  is limited at very small  $Q^2$  with  $Q^2 \equiv -q^2$  and  $q$  the four momentum transfer because there is no free pion target. The electromagnetic production of pion in  $ep \rightarrow en\pi^+$  is usually used to extract the EM form factor of pion [11–15]. It is a natural question that how large the TPE contributions in this process and how large their corrections to the extracted EM form factor of pion are. In this work, we estimate the TPE contributions in this process within the hadronic model and analyse the TPE corrections to the separated cross sections which are used to determine the EM form factor of pion.

We organize the paper as follows. In Sec. II we describe the basic formulas of our calculation under the pion dominance approximation, in Sec. III we express the physical amplitude as a sum of two invariant amplitudes and discuss the IR property of the TPE amplitude, in Sec. IV we express the unpolarized differential cross section by the coefficients of the invariant amplitudes, in Sec. V we present the numerical results for the TPE corrections to the amplitude, to the unpolarized differential cross section and to the separated cross section  $\sigma_{L,T,LT,TT}$ . The detailed discussion on these numerical results and the conclusion from these numerical results are also given.

## II. BASIC FORMULA FOR $ep \rightarrow en\pi^+$

Under the one-photon exchange (OPE) approximation, the  $ep \rightarrow en\pi^+$  process can be separated into two subprocesses  $e \rightarrow e\gamma^*$  and  $\gamma^*p \rightarrow n\pi^+$  showed in Fig. 1 where we label the momenta of initial electron, initial proton, final electron, final pion and final neutron as  $p_{1,2,3,4,5}$  and for simplicity we define the following five independent Lorentz invariant variables  $s \equiv (p_1 + p_2)^2$ ,  $Q^2 \equiv -(p_1 - p_3)^2$ ,  $W \equiv \sqrt{(p_4 + p_5)^2}$ ,  $t \equiv (p_2 - p_5)^2$  and  $p_{14} \equiv p_1 \cdot p_4$ .

The dynamics of the subprocess  $e \rightarrow e\gamma^*$  is clear while the dynamics of the subprocess  $\gamma^*p \rightarrow n\pi^+$  is very complex. In this work we limit our discussion on the momenta

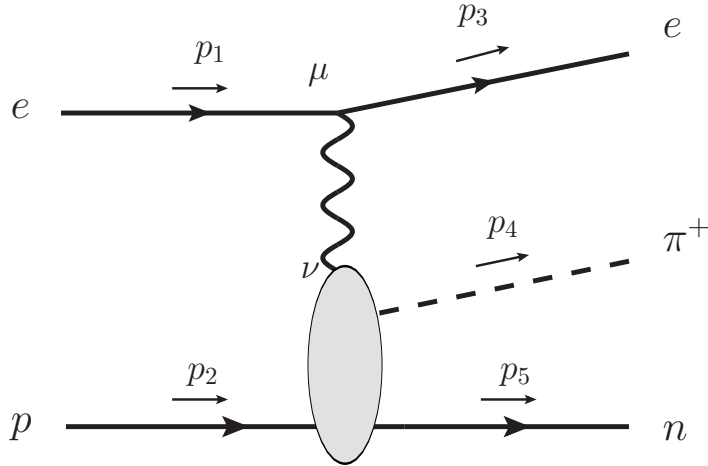


FIG. 1:  $ep \rightarrow en\pi^+$  under the one-photon exchange.

region with  $Q^2$  small,  $-t \sim 0$  and  $W$  far away from the resonances. In this region, one can estimate the subprocess  $\gamma^*p \rightarrow n\pi^+$  in the hadronic level as an approximation and can expect that the  $\pi$  exchange diagram showed in Fig. 2(a) may give the most important contribution due to the large enhancement from the pion propagator. In Fig. 2, the  $s$ -channel diagram is also presented to keep the gauge invariance. The unpolarized differential cross section at small  $-t$  is usually used to determine the EM form factor of pion. Different from  $e\pi^+ \rightarrow e\pi^+$  process where the EM form factor of pion can be extracted from the total cross section directly, the EM form factor can not be extracted directly from the unpolarized differential cross section of  $ep \rightarrow en\pi^+$  and should be extracted via the angle dependence of the unpolarized differential cross section. The TPE contributions may change the angle dependence of the unpolarized differential cross section and then effect the extraction of the EM form factor in an indirect and nontrivial way. When go to discuss the TPE effects, the contributions from the corresponding TPE diagrams showed in Fig. 3 should be considered.

We use the interactions constructed in Ref. [16] to describe the interactions between the pion and the photon. A little different from  $e\pi^+ \rightarrow e\pi^+$  process, to keep the gauge invariance the interactions between the photon and the proton should be also included. The interaction between pion, proton and neutron is simply taken as iso-scalar type.

When taking Feynman gauge and limiting the discussion on the small  $-t$ , the contri-

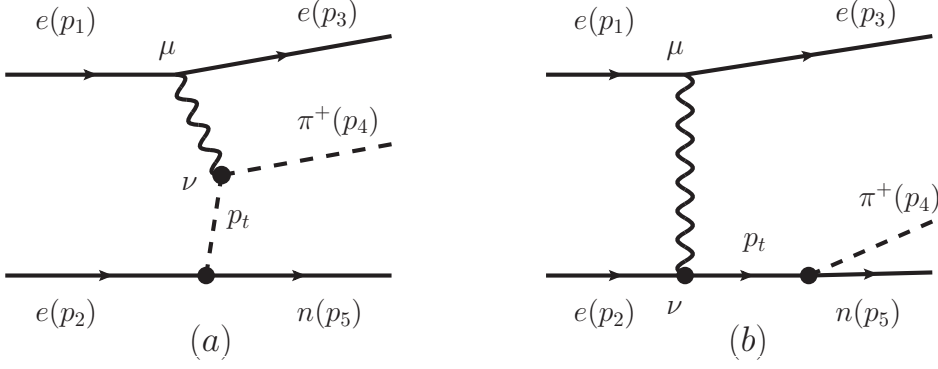


FIG. 2: Diagrams for  $ep \rightarrow en\pi^+$  under the one-photon exchange with (a) the pion exchange diagram and (b) the elastic  $s$ -channel diagram.

Contributions from the diagrams Fig. 2 (a) and Fig. 3 (a,b,c) are the most important in the OPE and TPE levels, respectively. Since we are only interested in the property of the TPE contributions or the ratio of the TPE contributions to the OPE contributions, in the following discussion we only consider the contributions from Fig. 2 (a) and Fig. 3(a,b,c). Such simplification has an advantage that the TPE contributions have a very simple form in the amplitude level.

Taking Feynmann gauge, one has

$$\begin{aligned}
\mathcal{M}_{1\gamma}^{(a)} &= -i\bar{u}_e(p_3)(-ie\gamma^\mu)u_e(p_1)\bar{u}_n(p_5)(-g_0\gamma_5)u_p(p_2)\Gamma^\nu(p_4, p_t)S_\pi(p_t)D_{\mu\nu}(p_1 - p_3), \\
\mathcal{M}_{2\gamma}^{(a)} &= -i\int\frac{d^4k_1}{(2\pi)^4}\bar{u}_e(p_3)(-ie\gamma^\mu)S_F(p_1 - k_1)(-ie\gamma^\rho)u_e(p_1)\bar{u}_n(p_5)(-g_0\gamma_5)u_p(p_2)\Gamma^\nu(p_4, p_4 - k_2) \\
&\quad S_\pi(p_4 - k_2)\Gamma^\omega(p_4 - k_2, p_t)S_\pi(p_t)D_{\mu\nu}(k_2)D_{\rho\omega}(k_1), \\
\mathcal{M}_{2\gamma}^{(b)} &= -i\int\frac{d^4k_1}{(2\pi)^4}\bar{u}_e(p_3)(-ie\gamma^\mu)S_F(p_1 - k_1)(-ie\gamma^\rho)u_e(p_1)\bar{u}_n(p_5)(-g_0\gamma_5)u_p(p_2)\Gamma^\omega(p_4, p_4 - k_1) \\
&\quad S_\pi(p_4 - k_1)\Gamma^\nu(p_4 - k_1, p_t)S_\pi(p_t)D_{\mu\nu}(k_2)D_{\rho\omega}(k_1), \\
\mathcal{M}_{2\gamma}^{(c)} &= -i\int\frac{d^4k_1}{(2\pi)^4}\bar{u}_e(p_3)(-ie\gamma^\mu)S_F(p_1 - k_1)(-ie\gamma^\rho)u_e(p_1)\bar{u}_n(p_5)(-g_0\gamma_5)u_p(p_2)\Lambda^{\omega\nu}(k_1, k_2)S_\pi(p_t) \\
&\quad D_{\mu\nu}(k_2)D_{\rho\omega}(k_1), \tag{1}
\end{aligned}$$

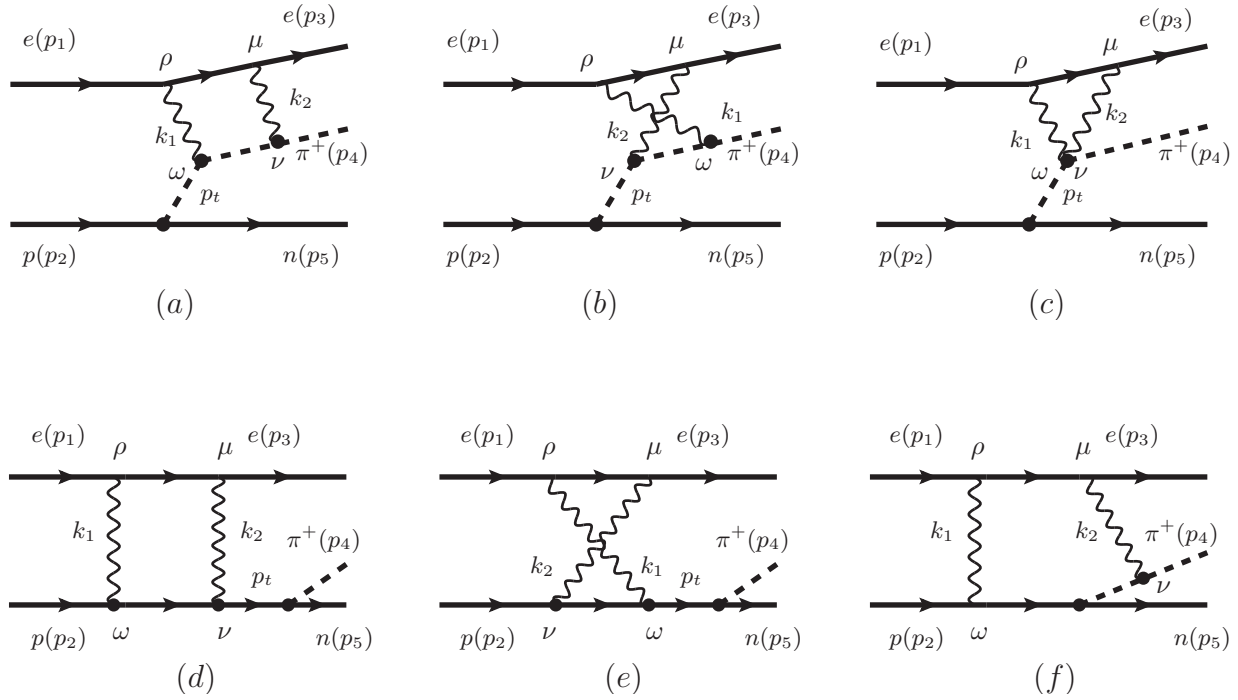


FIG. 3: Diagrams for  $ep \rightarrow en\pi^+$  with two-photon exchange where (a,b,c) are corresponding to the  $\pi$  exchange  $t$ -channel one-photon exchange diagram and (d,e,f) are corresponding to the  $s$ -channel one-photon exchange diagram.

with

$$\begin{aligned}
 S_F(q) &= \frac{i(\not{q} + m_e)}{q^2 - m_e^2 + i\epsilon}, \\
 S_\pi(q) &= \frac{i}{q^2 - m_\pi^2 + i\epsilon}, \\
 D_{\mu\rho}(q) &= \frac{-i}{q^2 + i\epsilon} g_{\mu\rho},
 \end{aligned} \tag{2}$$

and

$$\begin{aligned}
 \Gamma^\mu(p_f, p_i) &= ie \left[ (1 + f(q^2)q^2)(p_f + p_i)^\mu - f(q^2)(p_f^2 - p_i^2)q^\mu \right] \\
 \Lambda^{\mu\nu}(k_1, k_2) &= 2ie^2 \left[ g^{\mu\nu} + f(k_1^2)(k_1^\mu k_1^\nu - k_1^\mu k_1^\nu) + f(k_2^2)(k_2^\mu k_2^\nu - k_2^\mu k_2^\nu) \right],
 \end{aligned} \tag{3}$$

where  $e = -|e|$ ,  $q \equiv p_f - p_i$  and  $f(q^2)$  describes the EM form factor of pion  $F_\pi(q^2)$  and has the relation

$$F_\pi(q^2) = 1 + q^2 f(q^2). \tag{4}$$

### III. THE IR DIVERGENCE OF THE AMPLITUDE

Generally, the amplitudes given in Eq. (1) can be expressed in the following simple form.

$$\begin{aligned}\mathcal{M}_{1\gamma} &\equiv \mathcal{M}_{1\gamma}^{(a)} = c_1^{(1\gamma)} \mathcal{M}_1 + c_2^{(1\gamma)} \mathcal{M}_2, \\ \mathcal{M}_{2\gamma} &\equiv \mathcal{M}_{2\gamma}^{(a+b+c)} = c_1^{(2\gamma)} \mathcal{M}_1 + c_2^{(2\gamma)} \mathcal{M}_2,\end{aligned}\tag{5}$$

with

$$\begin{aligned}\mathcal{M}_1 &\equiv i\bar{u}(p_3, m_e)(2\not{p}_4 + \not{p}_3 - \not{p}_1)u(p_1, m_e) \bar{u}(p_5, m_n)\gamma_5 u(p_2, m_p), \\ \mathcal{M}_2 &\equiv i\bar{u}(p_3, m_e)u(p_1, m_e) \bar{u}(p_5, m_n)\gamma_5 u(p_2, m_p).\end{aligned}\tag{6}$$

The coefficients  $c_{1,2}^{(1\gamma)}$  can be easily gotten which are expressed as

$$\begin{aligned}c_1^{(1\gamma)} &= \frac{-4\pi\alpha_e g_0}{t - m_\pi^2} \left( \frac{1}{Q^2} - F_\pi(Q^2) \right), \\ c_2^{(1\gamma)} &= 0,\end{aligned}\tag{7}$$

with  $\alpha_e \equiv e^2/4\pi$ .

When taking the approximation  $m_e = 0$  one has  $c_2^{(2\gamma)} = 0$  due to the symmetry and our numerical results also show this property. The expressions for  $c_{1,2}^{(2\gamma)}$  are complex even the form factor  $f(k^2)$  is taken as a simple monopole form. A general property is that there is only IR divergence in  $c_1^{(2\gamma)}$ . The detailed analysis shows that the IR divergence comes from diagrams Fig. 3(a,b) and the corresponding pure IR divergence [17] in  $c_1^{(2\gamma)}$  in the dimensions regularization can be expressed as

$$\begin{aligned}c_{1,\text{IR}}^{(2\gamma,a)} &= \frac{-2\alpha_e^2 g_0 [Q^2 F_\pi(Q^2) - 1] a i\pi^2 \text{Log} \left[ \frac{m_\pi^2 - 2p_{14} - Q^2 - t + \sqrt{-4m_e^2 m_\pi^2 + a^2}}{2m_e m_\pi} \right]}{\pi^2 Q^2 (t - m_\pi^2) \sqrt{-4m_e^2 m_\pi^2 + a^2}}, \\ c_{1,\text{IR}}^{(2\gamma,b)} &= \frac{-4\alpha_e^2 g_0 p_{14} [Q^2 F_\pi(Q^2) - 1] i\pi^2 \text{Log} \left[ \frac{p_{14} + \sqrt{-m_e^2 m_\pi^2 + p_{14}^2}}{m_e m_\pi} \right]}{\pi^2 Q^2 (t - m_\pi^2) 2\sqrt{-m_e^2 m_\pi^2 + p_{14}^2}},\end{aligned}\tag{8}$$

with  $a \equiv 2p_{14} + Q^2 + t - m_\pi^2$ . The above IR divergence should be included in any experimental data analysis when the real radiative corrections are included.

In  $ep \rightarrow ep$  process, the contribution from the TPE diagrams under the soft momentum approximation which includes the IR divergence is usually estimated via the classical Tsai

and Mao's soft approximation [18] in the experimental analysis. In this approximation the soft TPE contribution is calculated by taking the momentum of one photon as zero both in the numerator and one of the denominators of the propagators. In Ref. [19], the authors suggest another approximation to estimate the soft TPE contribution. In their estimation, the soft contribution is calculated by taking momentum of one photon as zero only in the numerator. The analytical expressions in the latter method can be get in  $ep \rightarrow ep$  or  $e\pi \rightarrow e\pi$ . In  $ep \rightarrow en\pi^+$  process the intermediate pion is off-shell which introduces an additional variable  $t$ , the analytical expressions under the above soft approximation are very complex and we do not go to show them. In the practical calculation, we find that the difference between the soft contribution by Tsai and Mao method and the pure IR contribution given by Eq. (8) is small, while the difference between the soft contribution by Tjon method and the pure IR contribution is relatively large. For universality, in the following discussion we subtract the pure IR contribution from the full TPE contribution and define

$$c_{1,\text{fin}}^{(2\gamma)} \equiv c_1^{(2\gamma)} - (c_{1,\text{IR}}^{(2\gamma,a)} + c_{1,\text{IR}}^{(2\gamma,b)}). \quad (9)$$

#### IV. THE UNPOLARIZED CROSS SECTION

Using the general expression of the amplitudes Eq. (5) and Eq. (6), one can get the expressions of the unpolarized differential scattering cross sections as follows.

$$\begin{aligned} \frac{d^5\sigma_{un}^{1\gamma}}{dE_{e'}d\Omega_{e'}d\Omega_\pi} &\sim \sum_{spin} \mathcal{M}_{1\gamma}\mathcal{M}_{1\gamma}^* \\ &= 8|c_1^{(1\gamma)}|^2(-t) [8p_{14}^2 + 4(Q^2 + t - m_\pi^2)p_{14} - 2m_\pi^2Q^2], \\ \frac{d^5\sigma_{un}^{2\gamma}}{dE_{e'}d\Omega_{e'}d\Omega_\pi} &\sim \sum_{spin} 2\text{Re}[\mathcal{M}_{2\gamma}\mathcal{M}_{1\gamma}^*] \\ &= 2\text{Re}\left\{8c_1^{(1\gamma)}c_{1,\text{fin}}^{(2\gamma)}(-t) [8p_{14}^2 + 4(Q^2 + t - m_\pi^2)p_{14} - 2m_\pi^2Q^2] \right. \\ &\quad \left. + 8m_e c_1^{(1\gamma)}c_2^{(2\gamma)}(-t)(-m_\pi^2 + 4p_{14} + Q^2 + t)\right\}, \end{aligned} \quad (10)$$

where  $E_{e'}$  is the energy of final electron in the Lab frame,  $\Omega_{e'}$  is the angle of final electron in the Lab frame,  $\Omega_\pi$  is the angle of pion in the center frame of pion and final proton and

we have taken  $c_1^{(1\gamma)}$  as real. From Eq. (10) one can also see that the contribution from  $c_2^{(2\gamma)}$  can be neglected when taking the approximation  $m_e = 0$ .

The unpolarized cross sections above can be written as

$$\frac{d^5\sigma_{un}^X}{dE_{e'}d\Omega_{e'}d\Omega_\pi} \equiv \Gamma_\nu J(t, \phi_\pi \rightarrow \Omega_\pi) \frac{d^2\sigma_{un}^X}{dt d\phi_\pi}, \quad (11)$$

where  $X$  refers to  $1\gamma$  or  $2\gamma$ ,  $J(t, \phi_\pi \rightarrow \Omega_\pi) = \frac{dt}{\sin\theta_\pi d\theta_\pi}$  and  $\Gamma_\nu = \frac{\alpha_e}{2\pi^2} \frac{E_{e'}}{E_e} \frac{W^2 - m_p^2}{2m_p Q^2} \frac{1}{1-\epsilon}$  is the virtual photon flux factor with  $E_e$  the energy of initial electron in the Lab frame,  $m_p$  the mass of proton and  $\epsilon$  the longitudinal polarization of the virtual photon whose definition can be found in the Appendix. According to the dependence on  $\phi_\pi$  and  $\epsilon$ , the OPE cross section  $\frac{d^2\sigma_{un}^{1\gamma}}{dt d\phi_\pi}$  can be separated into four terms as follows.

$$\begin{aligned} 2\pi \frac{d^2\sigma_{un}^{1\gamma}}{dt d\phi_\pi} &= \epsilon \frac{d\sigma_L^{1\gamma}}{dt} + \frac{d\sigma_T^{1\gamma}}{dt} + \sqrt{2\epsilon(\epsilon+1)} \frac{d\sigma_{LT}^{1\gamma}}{dt} \cos\phi_\pi + \epsilon \frac{d\sigma_{TT}^{1\gamma}}{dt} \cos 2\phi_\pi, \\ &\equiv \epsilon\sigma_L^{1\gamma} + \sigma_T^{1\gamma} + \sqrt{2\epsilon(\epsilon+1)}\sigma_{LT}^{1\gamma} \cos\phi_\pi + \epsilon\sigma_{TT}^{1\gamma} \cos 2\phi_\pi \end{aligned} \quad (12)$$

where the four separated cross sections  $d\sigma_{L,T,LT,TT}^{1\gamma}/dt$  shortly written as  $\sigma_{L,T,LT,TT}^{1\gamma}$  are only depend on  $Q^2$ ,  $W$  and  $\theta_\pi$ .

When one takes  $m_e = 0$  in Eq. (10), one can see that the TPE cross section  $\frac{d^2\sigma_{un}^{2\gamma}}{dt d\phi_\pi}$  has the same form with OPE cross section. After using the variables  $Q^2$ ,  $W$ ,  $\epsilon$ ,  $\theta_\pi$  and  $\phi_\pi$  to express the cross section one can see that  $\frac{d^2\sigma_{un}^{2\gamma}}{dt d\phi_\pi}$  has the same  $\phi_\pi$  dependence with  $\frac{d^2\sigma_{un}^{1\gamma}}{dt d\phi_\pi}$  and can also be separated into the same form as Eq. (12) but now the four corresponding separated cross sections  $\sigma_{L,T,LT,TT}^{2\gamma}$  are dependent on  $Q^2$ ,  $W$ ,  $\theta_\pi$  and  $\epsilon$ .

## V. THE NUMERICAL RESULTS AND DISCUSSION

In the practical calculation, we take the input form factor  $F_\pi(q^2)$  as the monopole from which is used in [20] and [16].

$$F_\pi(q^2) = \frac{-\Lambda^2}{q^2 - \Lambda^2}, \quad (13)$$

with  $\Lambda = 0.77\text{GeV}$ . We use the packages FEYNALC [21] and LOOPTOOLS [22] to carry out the analytical and numerical calculations, respectively. For comparison, we take the experiment kinematics in JLab  $F_\pi$  [14] with  $Q^2 = 1 \text{ GeV}^2$  and  $Q^2 = 1.6 \text{ GeV}^2$  at  $W = 1.95 \text{ GeV}^2$  as examples to show the TPE contributions.



### A. TPE contributions to the amplitude $c_{1,\text{fin}}^{(2\gamma)}/c_1^{(1\gamma)}$

The  $-t$  dependence of the TPE correction  $\text{Re}[c_{1,\text{fin}}^{(2\gamma)}/c_1^{(1\gamma)}]$  is presented in Fig. 4 where the left and right panels are corresponding to  $Q^2 = 1 \text{ GeV}^2$  and  $Q^2 = 1.6 \text{ GeV}^2$ , respectively. The (blue) dashed curves and the (olive) dash-dotted curves refer to the results at  $\phi_\pi = \pi/6$  and  $\phi_\pi = \pi/3$  with  $\epsilon = 0.65$  or  $0.63$ , the (black) solid curves and the (red) dotted curves are associated with  $\epsilon = 0.33$  or  $0.27$ . The results clearly show that the absolute magnitude of TPE corrections  $\text{Re}[c_{1,\text{fin}}^{(2\gamma)}/c_1^{(1\gamma)}]$  at  $\phi_\pi = \pi/6$  increase when  $-t$  increases while the corrections at  $\phi_\pi = \pi/3$  are not sensitive on  $-t$ . Another interesting property is that the TPE corrections at very small  $-t$  are not sensitive on  $\phi_\pi$  while the TPE corrections at large  $-t$  are sensitive on  $\phi_\pi$ .

At  $\phi_\pi = \pi/6$ , one can see that the TPE corrections at small  $\epsilon$  are about  $-4\% \sim -6\%$  at small  $-t$  and reach about  $-7\% \sim -10\%$  at large  $-t$  for  $Q^2 = 1.0$  and  $1.6 \text{ GeV}^2$ , respectively. The magnitude at small  $-t$  and small  $\epsilon$  is similar with the TPE corrections in  $e\pi \rightarrow e\pi$ . These properties suggest that the  $-t$  dependence of the TPE corrections at small  $\phi_\pi$  is relatively important.

The  $-t$  dependence of the imaginary parts of the TPE corrections  $\text{Im}[c_{1,\text{fin}}^{(2\gamma)}/c_1^{(1\gamma)}]$  is presented in Fig. 5 where the same definitions with Fig. 4 are used for the curves. The results show an interesting and important property: the TPE corrections to the imaginary part are not sensitive on  $Q^2, \phi_\pi, -t$  and  $\epsilon$  at  $W = 1.95 \text{ GeV}$  and are almost about  $7\%$ .

The  $\epsilon$  dependence of the TPE corrections  $\text{Re}[c_{1,\text{fin}}^{(2\gamma)}/c_1^{(1\gamma)}]$  is presented in Fig. 6 where  $\theta_\pi$  is taken as  $\pi/18, \pi/12$  and  $-t$  is limited within the experimental data sets. The (black) solid curves and the (red) dotted curves refer to the results with  $\theta_\pi = \pi/18$  at  $Q^2 = 1$  and  $1.6 \text{ GeV}^2$ , respectively. The (blue) dashed curves and the (olive) dash-dotted curves are associated with  $\theta_\pi = \pi/12$ . The results clearly show that the absolute magnitude of  $\text{Re}[c_{1,\text{fin}}^{(2\gamma)}/c_1^{(1\gamma)}]$  decreases when  $\epsilon$  increases. This is a general property of the TPE corrections. At  $\epsilon = 0.1$  the TPE corrections  $\text{Re}[c_{1,\text{fin}}^{(2\gamma)}/c_1^{(1\gamma)}]$  reach about  $-9\%$  and  $-12\%$  at  $Q^2 = 1 \text{ GeV}^2$  and  $1.6 \text{ GeV}^2$ , respectively. The results in the right panel clearly show that the TPE corrections to the imaginary part are not sensitive on  $\epsilon$ .

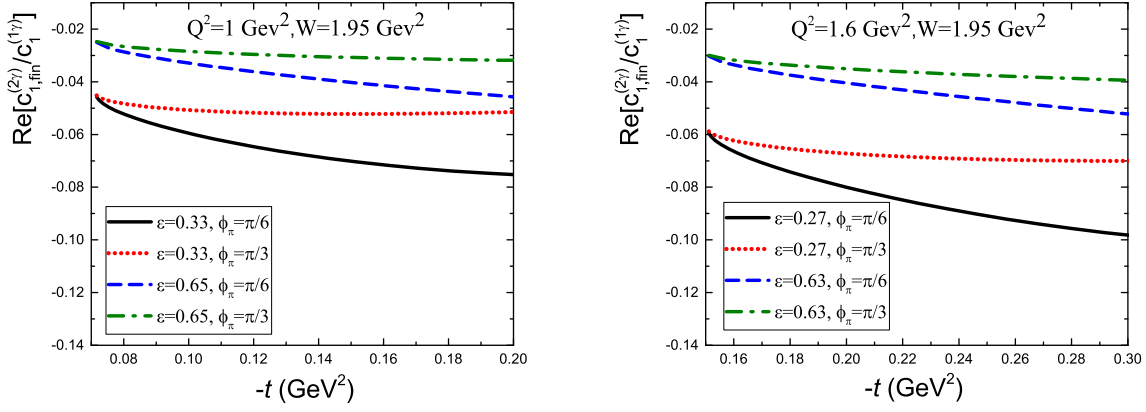


FIG. 4: Numeric results for  $\text{Re}[c_{1,\text{fin}}^{(2\gamma)}/c_1^{(1\gamma)}]$  vs.  $-t$  at fixed  $Q^2$ ,  $W$ ,  $\epsilon$  and  $\phi_\pi$ . The left panel is the result with  $Q^2 = 1 \text{ GeV}^2$  and the right panel is the result with  $Q^2 = 1.6 \text{ GeV}^2$ .

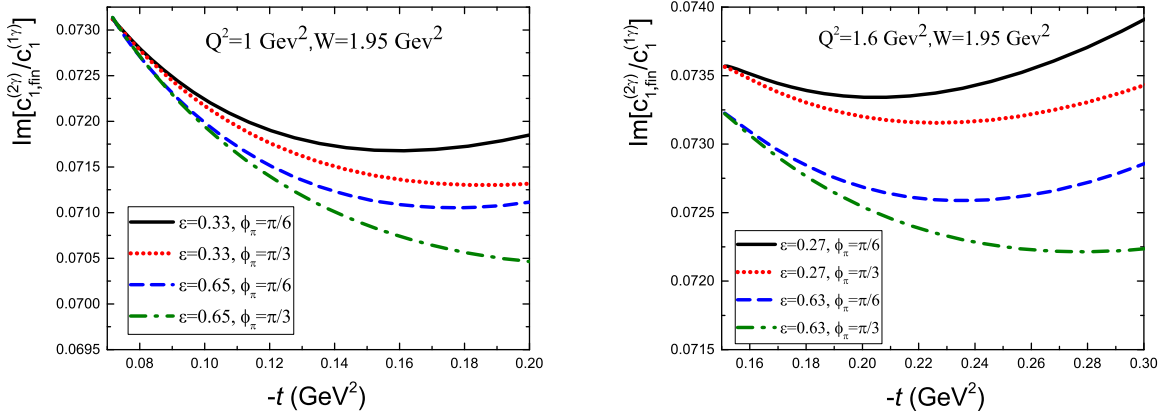


FIG. 5: Numeric results for  $\text{Im}[c_{1,\text{fin}}^{(2\gamma)}/c_1^{(1\gamma)}]$  vs.  $-t$  at fixed  $Q^2$ ,  $W$ ,  $\epsilon$  and  $\phi_\pi$ . The left panel is the result with  $Q^2 = 1 \text{ GeV}^2$  and the right panel is the result with  $Q^2 = 1.6 \text{ GeV}^2$ .

## B. TPE corrections to unpolarized differential cross section

To show the TPE corrections to the unpolarized differential scattering cross section, we define

$$\delta_{un}^{2\gamma} \equiv \frac{d\sigma_{un}^{2\gamma}}{dt d\phi_\pi} / \frac{d\sigma_{un}^{1\gamma}}{dt d\phi_\pi} = \frac{2 \text{Re}[c_1^{(1\gamma)} c_{1,\text{fin}}^{(2\gamma)}]}{|c_1^{(1\gamma)}|^2} = 2 \text{Re}\left[\frac{c_{1,\text{fin}}^{(2\gamma)}}{c_1^{(1\gamma)}}\right], \quad (14)$$

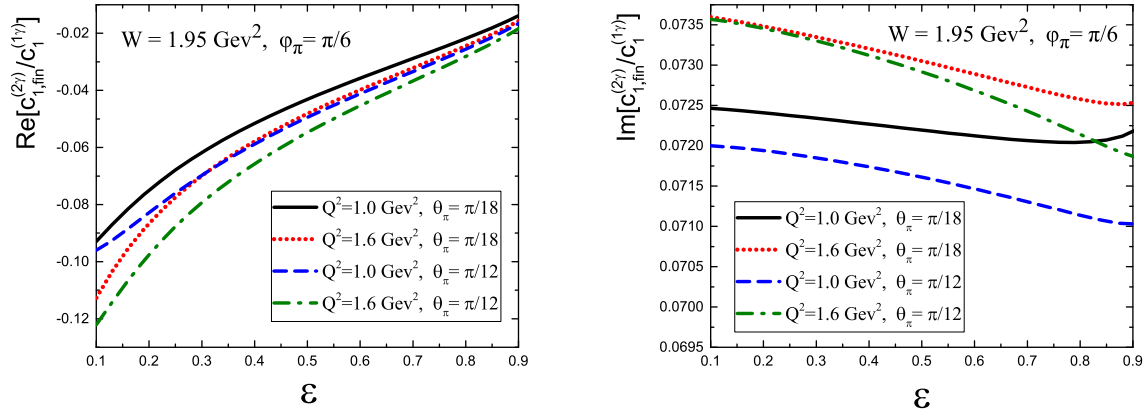


FIG. 6: Numeric results for  $c_{1,\text{fin}}^{(2\gamma)}/c_1^{(1\gamma)}$  vs.  $\epsilon$  at fixed  $Q^2, W, \theta_\pi$  and  $\phi_\pi$ . The left panel is the result for the real part and the right panel is the result for the imaginary part.

where we have used the property that  $c_1^{1\gamma}$  is real. Eq. (14) means that the TPE corrections to the unpolarized cross sections are just 2 times of the real part of the TPE corrections to the coefficient  $c_1$ . After considering this factor 2, one can see that the TPE corrections to the unpolarized cross section at small  $\epsilon$ , small  $\phi_\pi$  and  $Q = 1 \text{ GeV}^2$  can reach about  $-10\%$  which is not small. Furthermore, the TPE corrections are sensitive on  $\epsilon$ ,  $\phi_\pi$  and  $-t$  or  $\theta_\pi$  when  $Q^2$  and  $W$  are fixed. Generally one can expect that these two properties may result in nontrivial effects when extracting some physical quantities from the angle dependence of differential cross section.

When Comparing with the TPE corrections in  $e^+e^- \rightarrow p\bar{p}$  [7],  $e\pi \rightarrow e\pi$  [8],  $\mu p \rightarrow \mu p$  [9], and  $ep \rightarrow e\Delta \rightarrow ep\pi^0$  at  $W = 1232 \text{ GeV}$  [10], we can see that the absolute magnitude of the TPE correction in  $ep \rightarrow en\pi^+$  are much larger. This property can be understood by the fact that the intermediate pion with four momentum  $p_t \equiv p_5 - p_2$  is off-shell which is different from the other processes. Naively if  $p_t^2 = t$  goes to  $m_\pi^2$ , the TPE corrections to the coefficients should be same with the TPE corrections in the physical process  $e\pi \rightarrow e\pi$ . From Fig. 4, one can see that the absolute magnitude of TPE corrections  $\text{Re}[c_{1,\text{fin}}^{(2\gamma)}/c_1^{(1\gamma)}]$  decreases when  $t$  increases.

### C. TPE corrections to separated cross sections $\sigma_L, \sigma_T, \sigma_{LT}$ and $\sigma_{TT}$

Experimentally, the separated cross sections  $\sigma_L, \sigma_T, \sigma_{LT}$  and  $\sigma_{TT}$  are usually extracted from the original experimental data  $\frac{d\sigma_{un}^{Ex}}{dt d\phi_\pi}$  via Eq. (12) and then are used to determine the EM form factor of  $\pi^+$ . Since the TPE corrections to the unpolarized cross section are not small and sensitive on the angles, one should be careful in the separation. In this section, we analysis the TPE corrections to the separated cross sections.

When considering the TPE contribution, one has

$$\frac{d\sigma_{un}^{Ex}}{dt d\phi_\pi} = \frac{d\sigma_{un}^{ph,1\gamma}}{dt d\phi_\pi} (1 + \delta_{un}^{ph,2\gamma}), \quad (15)$$

where  $\frac{d\sigma_{un}^{Ex}}{dt d\phi_\pi}$  refers to the experimental observed cross section,  $\frac{d\sigma_{un}^{ph,1\gamma}}{dt d\phi_\pi}$  refers to the physical cross section via OPE, and  $\delta_{un}^{ph,2\gamma}$  refers to the physical TPE correction to the cross section. Since actually we don't know all the dynamics of QCD, the physical  $\frac{d\sigma_{un}^{ph,1\gamma}}{dt d\phi_\pi}$  and  $\delta_{un}^{ph,2\gamma}$  are difficult to be calculated precisely. While it is a good approximation to assume  $\delta_{un}^{ph,2\gamma} \approx \delta_{un}^{2\gamma}$  since the most important contributions in the OPE and TPE levels are considered in our calculation, respectively. We can expect that the model dependence of their ratio is much weaker than the absolute magnitude like the  $ep \rightarrow ep$  case where the relative TPE corrections are not sensitive on the input form factors. By this approximation, we have

$$\frac{d\bar{\sigma}_{un}^{Ex}}{dt d\phi_\pi} \equiv \frac{d\sigma_{un}^{ph,1\gamma}}{dt d\phi_\pi} \approx \frac{d\sigma_{un}^{Ex}}{dt d\phi_\pi} (1 - \delta_{un}^{2\gamma}). \quad (16)$$

The current experimental analysis is based the experimental cross section  $\frac{d\sigma_{un}^{Ex}}{dt d\phi_\pi}$  and Eq. (12). After considering the TPE contributions, in principle the analysis should be based on the corrected experimental cross section  $\frac{d\bar{\sigma}_{un}^{Ex}}{dt d\phi_\pi}$  and Eq. (12). The comparison between the results from these two analysis can tell us how large the TPE corrections to the separated cross sections  $\sigma_L, \sigma_T, \sigma_{LT}$  and  $\sigma_{TT}$  are.

In the practical analysis, we take two data sets named as ExA and ExB as inputs to do the analysis. In the data sets ExA, we take the experimental extracted  $\sigma_L^{\text{ExA}}, \sigma_T^{\text{ExA}}, \sigma_{LT}^{\text{ExA}}$  and  $\sigma_{TT}^{\text{ExA}}$  by JLab  $F_\pi$  [14] as inputs to get  $\frac{d\sigma_{un}^{\text{ExA}}}{dt d\phi_\pi}$  at specific  $\epsilon$  and  $\phi_\pi$  via Eq. (12). The corresponding values are listed in Table. I. We take  $\epsilon$  as 0.33, 0.66 at the low  $Q^2$ , take  $\epsilon$  as 0.27, 0.63 at the high  $Q^2$  and take  $\phi_\pi$  from  $5^\circ$  to  $355^\circ$  with  $\Delta\phi_\pi = 25^\circ$ . In the data sets ExB, we use the experimental fitted formula [14] to produce  $\frac{d\sigma_{un}^{\text{ExB}}}{dt d\phi_\pi}$ . For comparison,

$Q^2(\text{GeV}^2)$	$W(\text{GeV})$	$t(\text{GeV}^2)$	$\sigma_L^{\text{ExA}}$	$\sigma_T^{\text{ExA}}$	$\sigma_{LT}^{\text{ExA}}$	$\sigma_{TT}^{\text{ExA}}$
0.945	1.970	-0.080	11.840	6.526	1.339	-1.584
1.010	1.943	-0.100	9.732	5.656	0.719	-0.582
1.050	1.926	-0.120	7.116	5.926	0.331	-1.277
1.067	1.921	-0.140	4.207	5.802	0.087	-0.458
1.532	1.975	-0.165	4.378	3.507	0.356	-0.268
1.610	1.944	-0.195	3.191	3.528	0.143	-0.126
1.664	1.924	-0.225	2.357	2.354	-0.028	-0.241
1.702	1.911	-0.255	2.563	2.542	-0.100	-0.083

TABLE I: Numerical results for the separated cross sections  $\sigma_L^{\text{ExA}}, \sigma_T^{\text{ExA}}, \sigma_{LT}^{\text{ExA}}, \sigma_{TT}^{\text{ExA}}$  directly taken from JLab  $F_\pi$  [14].

$Q^2(\text{GeV}^2)$	$W(\text{GeV})$	$t(\text{GeV}^2)$	$\sigma_L^{\text{ExB}}$	$\sigma_T^{\text{ExB}}$	$\sigma_{LT}^{\text{ExB}}$	$\sigma_{TT}^{\text{ExB}}$
0.945	1.970	-0.080	11.8344	6.8054	1.0266	-0.8270
1.010	1.943	-0.100	8.4637	5.9616	0.5703	-0.8978
1.050	1.926	-0.120	6.0577	5.3624	0.0985	-1.0413
1.067	1.921	-0.140	4.2969	4.9353	-0.0427	-1.2690
1.532	1.975	-0.165	4.6398	3.7839	0.3938	-0.1479
1.610	1.944	-0.195	3.3657	3.3617	0.1901	-0.1395
1.664	1.924	-0.225	2.4370	3.0447	0.0299	-0.1460
1.702	1.911	-0.255	1.7574	2.7978	-0.0997	-0.1569

TABLE II: Numerical results for the separated cross sections  $\sigma_L^{\text{ExA}}, \sigma_T^{\text{ExA}}, \sigma_{LT}^{\text{ExA}}, \sigma_{TT}^{\text{ExA}}$  produced by the fitted formulaes given in [14].

the corresponding  $\sigma_L^{\text{ExB}}, \sigma_T^{\text{ExB}}, \sigma_{LT}^{\text{ExB}}$  and  $\sigma_{TT}^{\text{ExB}}$  are listed in Table. II. In this data sets, we take  $\epsilon$  from 0.33 to 0.65 with  $\Delta\epsilon = 0.03$  at the low  $Q^2$ , take  $\epsilon$  from 0.27 to 0.62 with  $\Delta\epsilon = 0.035$  at the high  $Q^2$  to produce more data points, we also take  $\phi_\pi$  from  $5^\circ$  to  $355^\circ$  with  $\Delta\phi_\pi = 25^\circ$ .

After getting the data sets  $\frac{d\sigma_{un}^{\text{ExA,ExB}}}{dt d\phi_\pi}$ , we use the estimated TPE corrections in the

corresponding kinematics region to get  $\frac{d\sigma_{un}^{\text{ExA,ExB}}}{dt d\phi_\pi}$ . Then we use Eq. (12) to fit the corrected data sets to get the corrected separated cross sections  $\bar{\sigma}_L^{\text{ExA,ExB}}$ ,  $\bar{\sigma}_T^{\text{ExA,ExB}}$ ,  $\bar{\sigma}_{LT}^{\text{ExA,ExB}}$  and  $\bar{\sigma}_{TT}^{\text{ExA,ExB}}$ .

$Q^2(\text{GeV}^2)$	$W(\text{GeV})$	$t(\text{GeV}^2)$	$\bar{\sigma}_L^{\text{ExA}}/\sigma_L^{\text{ExA}}$	$\bar{\sigma}_T^{\text{ExA}}/\sigma_T^{\text{ExA}}$	$\bar{\sigma}_{LT}^{\text{ExA}}/\sigma_{LT}^{\text{ExA}}$	$\bar{\sigma}_{TT}^{\text{ExA}}/\sigma_{TT}^{\text{ExA}}$
0.945	1.970	-0.080	0.9209	1.2064	1.2046	1.0024
1.010	1.943	-0.100	0.9137	1.2104	1.3394	0.8963
1.050	1.926	-0.120	0.8726	1.1977	1.7029	0.9777
1.067	1.921	-0.140	0.7820	1.1858	3.5629	0.7903
1.532	1.975	-0.165	0.8518	1.2312	1.4101	0.8833
1.610	1.944	-0.195	0.7839	1.2273	1.9492	0.6490
1.664	1.924	-0.225	0.7095	1.2269	-3.5338	0.8344
1.702	1.911	-0.255	0.7946	1.2453	-0.1846	0.3141

TABLE III: Numerical results for the ratios  $\bar{\sigma}_X^{\text{ExA}}/\sigma_X^{\text{ExA}}$  where X refers to L, T, LT and TT.

$Q^2(\text{GeV}^2)$	$W(\text{GeV})$	$t(\text{GeV}^2)$	$\bar{\sigma}_L^{\text{ExB}}/\sigma_L^{\text{ExB}}$	$\bar{\sigma}_T^{\text{ExB}}/\sigma_T^{\text{ExB}}$	$\bar{\sigma}_{LT}^{\text{ExB}}/\sigma_{LT}^{\text{ExB}}$	$\bar{\sigma}_{TT}^{\text{ExB}}/\sigma_{TT}^{\text{ExB}}$
0.945	1.970	-0.080	0.9191	1.2027	1.2730	0.9470
1.010	1.943	-0.100	0.8967	1.1990	1.4263	0.9554
1.050	1.926	-0.120	0.8664	1.1932	3.0947	0.9711
1.067	1.921	-0.140	0.8243	1.1853	0.5850	0.9917
1.532	1.975	-0.165	0.8510	1.2278	1.4284	0.6491
1.610	1.944	-0.195	0.8083	1.2275	1.7674	0.6349
1.664	1.924	-0.225	0.7490	1.2271	5.4036	0.6333
1.702	1.911	-0.255	0.6669	1.2267	-0.2142	0.6378

TABLE IV: Numerical results for the ratios  $\bar{\sigma}_X^{\text{ExB}}/\sigma_X^{\text{ExB}}$  where X refers to L, T, LT and TT.

In Table III and IV, we present the relative TPE corrections  $\bar{\sigma}_X^{\text{ExA}}/\sigma_X^{\text{ExA}}$  and  $\bar{\sigma}_X^{\text{ExB}}/\sigma_X^{\text{ExB}}$  where X refers to L, T, LT and TT. The numerical results show a general property that both the two data sets give similar relative TPE corrections to  $\sigma_{L,T,TT}^{\text{ExA,ExB}}$  and give very different relative TPE corrections to  $\sigma_{LT}^{\text{ExA,ExB}}$  at some special points. The latter can

be understood in a simple way since in these points the input data sets  $\sigma_{LT}^{\text{ExA,ExB}}$  are much smaller than the others. This means that the relative uncertainty to the extracted  $\sigma_{LT}^{\text{ExA,ExB}}$  actually is much larger than others.

At  $Q^2 \approx 1 \text{ GeV}^2$  and  $-t \approx 0.1 \text{ GeV}^2$ , the relative TPE corrections to  $\sigma_L^{\text{ExA,ExB}}$  are about  $-10\%$  and the corrections to  $\sigma_T^{\text{ExA,ExB}}$  are about  $20\%$ . When  $Q^2$  and  $-t$  increase, the relative TPE corrections to  $\sigma_L^{\text{ExA,ExB}}$  reach about  $-20\% \sim -30\%$ , while are still about  $20\%$  to  $\sigma_T^{\text{ExA,ExB}}$ . The relative TPE corrections to  $\sigma_{TT}^{\text{ExA,ExB}}$  are small at small  $-t$ , while are large and sensitive on the input data sets at large  $-t$ . the TPE corrections to  $\sigma_{LT}^{\text{ExA,ExB}}$  are always large and even become un-reliable and very sensitive on the input data sets at large  $-t$ . The experimental extracted  $\sigma_L$  is usually used to determine the pion form factor  $F_\pi$  through the Chew-Low method (based on the born term model [23]) or the Regge model [24]. Our results show that the relative TPE corrections to  $\sigma_L^{\text{ExA,ExB}}$  reach about  $-10\% \sim -30\%$  at  $Q^2 = 1 \sim 1.6 \text{ GeV}^2$ . This means the relative TPE corrections to the EM form factor of pion are about at the order  $-5\% \sim -15\%$  and should be considered carefully. At high  $Q^2$ , one can expect the TPE corrections should be much more important and should be considered seriously to extract the EM form factor of pion reliably.

In summary, in this work the TPE corrections to the amplitude and the unpolarized differential cross section of  $ep \rightarrow en\pi^+$  are estimated in a hadronic model. The TPE corrections to the extracted four separated cross sections are also analysed based on the experimental data sets. Our results show that at  $Q^2 = 1 \sim 1.6 \text{ GeV}^2$  the TPE correction to  $\sigma_L$  is about  $-10\% \sim -30\%$ , and about  $20\%$  to  $\sigma_T$ .

## VI. ACKNOWLEDGMENTS

The author Hai-Qing Zhou would like to thank Zhi-Yong Zhou and Dian-Yong Chen for their kind and helpful discussions. This work is supported by the National Natural Science Foundations of China under Grant No. 11375044.

**VII. APPENDIX: THE MOMENTA IN THE LAB FRAME AND CENTER  
FRAME OF  $n\pi^+$**

In this appendix, we list the manifest expressions of the momenta used in our calculation in the Lab frame and the center frame of  $n\pi^+$ . In the center frame of pion ( $p_4$ ) and neutron ( $p_5$ ), the momenta labelled as  $p_{iC}$  are taken as

$$\begin{aligned}
p_{1C} &= (E_{1C}, E_{1C}\sin\theta_1, 0, E_{1C}\cos\theta_1), \\
p_{2C} &= (E_{2C}, 0, 0, -\sqrt{E_{2C}^2 - M_n^2}), \\
p_{45C} &\equiv p_{4C} + p_{5C} = (W, 0, 0, 0), \\
q_C &\equiv p_{45C} - p_{2C} = (W - E_{2C}, 0, 0, \sqrt{E_{2C}^2 - M_n^2}), \\
p_{3C} &= p_{1C} - q_C, \\
p_{4C} &= (E_{\pi C}, p_{\pi C}\sin\theta_\pi\cos\phi_\pi, p_{\pi C}\sin\theta_\pi\sin\phi_\pi, p_{\pi C}\cos\theta_\pi), \\
p_{5C} &= p_{45C} - p_{4C}.
\end{aligned} \tag{17}$$

In the lab frame the momenta labelled as  $p_{iL}$  are taken as

$$\begin{aligned}
p_{1L} &= (E_e, 0, 0, E_e), \\
p_{2L} &= (m_p, 0, 0, 0), \\
p_{3L} &= (E_{e'}, E_{e'}\sin\theta_{e'}, 0, E_{e'}\cos\theta_{e'}).
\end{aligned} \tag{18}$$

From these expressions, we have the following relations.

$$\begin{aligned}
s &= \frac{1}{2} \left[ m_p^2 + Q^2 + W^2 + \frac{\sqrt{((m_p^2 + Q^2)^2 + 2(-m_p^2 + Q^2)W^2 + W^4)(1 - \epsilon^2)}}{1 - \epsilon} \right], \\
t &= \frac{1}{2W^2} \left[ -m_p^4 + (m_\pi^2 - W^2)(Q^2 + W^2) + m_p^2(m_\pi^2 - Q^2 + 2W^2) \right. \\
&\quad \left. + t_0\sqrt{m_p^4 + 2m_p^2(Q^2 - W^2) + (Q^2 + W^2)^2\cos\theta_\pi} \right], \\
p_{14} &= \frac{1}{4W^2} \left\{ \frac{t_0[-(m_p^2 + Q^2)t_1 + W^2t_2]\cos\theta_\pi}{\sqrt{m_p^4 + 2m_p^2(Q^2 - W^2) + (Q^2 + W^2)^2}} + t_1(m_p^2 - m_\pi^2 - W^2) \right. \\
&\quad \left. + 2Wt_0t_1 \sqrt{\frac{-Q^2t_1s + Q^2(m_p^2 - s)W^2}{[(m_p^2 + Q^2)^2 + 2(-m_p^2 + Q^2)W^2 + W^4]}} \sin\theta_\pi\cos\phi_\pi \right\},
\end{aligned} \tag{19}$$



with

$$\begin{aligned}
t_0 &= \sqrt{(m_p - m_\pi - W)(m_p + m_\pi - W)(m_p - m_\pi + W)(m_p + m_\pi + W)}, \\
t_1 &= m_p^2 + Q^2 - s, \\
t_2 &= m_p^2 - Q^2 - s.
\end{aligned} \tag{20}$$

and

$$\epsilon \equiv \left[ 1 + \frac{m_p^4 + 2m_p^2(Q^2 - W^2) + (Q^2 + W^2)^2}{2m_p^2 Q^2} \tan^2 \frac{\theta'_e}{2} \right]^{-1}. \tag{21}$$

The expressions of the kinematics are consistent with those used in JLab  $F_\pi$  experiment [14].

- 
- [1] P. G. Blunden, W. Melnitchuk, and J. A. Tjon, Phys. Rev.Lett. **91**, 142304 (2003); S. Kondratyuk, P. G. Blunden, W. Melnitchuk, and J. A.Tjon, Phys. Rev. Lett. **95**, 172503 (2005); P. G. Blunden, W. Melnitchuk, and J. A. Tjon, Phys. Rev. C **72**, 034612 (2005).
  - [2] Y. C. Chen, A. Afanasev, S. J. Brodsky, C. E. Carlson, and M. Vanderhaeghen, Phys. Rev. Lett. **93**, 122301 (2004); A. Afanasev, S. J. Brodsky, C. E. Carlson, Y. C. Chen, and M. Vanderhaeghen, Phys. Rev. D **72**, 013008 (2005).
  - [3] N. Kivel and M. Vanderhaeghen, Phys. Rev. Lett. **103**, 092004 (2009); D. Borisyyuk and A. Kobushkin, Phys. Rev. C **79**, 034001 (2009).
  - [4] D. Borisyyuk and A. Kobushkin, Phys. Rev. C **74**, 065203 (2006); D. Borisyyuk and A. Kobushkin, Phys. Rev. C **78**, 025208 (2008); D. Borisyyuk and A. Kobushkin, Phys. Rev. C **83**, 025203 (2011); D. Borisyyuk and A. Kobushkin, Phys. Rev. C **86**, 055204 (2012); D. Borisyyuk and A. Kobushkin, Phys. Rev. C **89**, 025204 (2014); P. G. Blunden and W. Melnitchouk, Phys. Rev. C **95**, 065209 (2017).
  - [5] N. Kivel and M. Vanderhaeghen, J. High Energy Phys. **04**, 029 (2013).
  - [6] Y. C. Chen, C. W. Kao, and S. N. Yang, Phys. Lett. B **652**, 269 (2007); D. Borisyyuk and A. Kobushkin, Phys. Rev. C **76**, 022201 (2007).
  - [7] D. Y. Chen, H. Q. Zhou, Y.B. Dong, Phys. Rev. C **78**, 045208 (2008).

- [8] P.G. Blunden, W. Melnitchouk, and J. A. Tjon, Phys. Rev. C **81**, 018202 (2010); Yu Bing Dong and S. D. Wanga, Phys. Lett. B **684**, 123 (2010).
- [9] Dian-Yong Chen and Yu-Bing Dong, Phys. Rev. C **87**, 045209,(2013); O. Tomalak and M. Vanderhaeghen, Phys. Rev. D **90**, 013006,(2014); O. Koshchii and A. Afanasev, Phys. Rev. D **94**, 116007 (2016); Hai-Qing Zhou, Phys. Rev. C **95**, 025203,(2017).
- [10] Hai-Qing Zhou and Shin Nan Yang, Phys. Rev. C **96**, 055210 (2017).
- [11] C. J. Bebek *et al.*, Phys. Rev. D **13**, 25 (1976); C. J. Bebek *et al.*, Phys. Rev. D **17**, 1693 (1978).
- [12] P. Brauel *et al.* (DESY), Phys. Lett. B **65**, 184 (1976); P. Brauel *et al.*, Phys. Lett. B **69**, 253 (1977); H. Ackermann *et al.*, Nucl. Phys. B **137**, 294 (1978); P. Brauel *et al.*, Z. Phys. C **3**, 101 (1979).
- [13] J. Volmer *et al.* (Jefferson Lab F $\pi$  Collaboration), Phys. Rev. Lett. **86**, 1713 (2001); T. Horn *et al.* (Jefferson Lab F $\pi$  Collaboration), Phys. Rev. Lett. **97**, 192001 (2006); V. Tadevosyan *et al.* (Jefferson Lab F $\pi$  Collaboration), Phys. Rev. C **75**, 055205 (2007).
- [14] H. P. Blok, T. Horn *et al.* (Jefferson Lab F $\pi$  Collaboration), Phys. Rev. C **78**, 045202 (2008).
- [15] G.M. Huber, *et al.* (Jefferson Lab F $\pi$  Collaboration), Phys. Rev. C **78**, 045203 (2008).
- [16] Hai Qing Zhou, Phys. Lett. B **706**, 82-85, (2011).
- [17] H. H. Patel, Comput. Phys. Commun. **197**, 276-290, (2015).
- [18] L. W. Mo and Y. S. Tsai, Rev. Mod. Phys. **41**, 205 (1969); Y. S. Tsai, Phys. Rev. **122**, 1898 (1961).
- [19] L. C. Maximon and J. A. Tjon, Phys. Rev. C **62**, 054320 (2000).
- [20] P. G. Blunden, W. Melnitchouk, J. A. Tjon, Phys. Rev. C **81**, 018202 (2010).
- [21] Vladyslav Shtabovenko, Rolf Mertig and Frederik Orellana, Comput. Phys. Commun. **207**, 432 (2016); R. Mertig, M. Bohm and Ansgar Denner, Comput. Phys. Commun. **64**, 345 (1991).
- [22] T. Hahn, M. Perez-Victoria, Comput. Phys. Commun. **118**, 153 (1999).
- [23] A. Actor, J. G. Korner, and I. Bender, Nuovo Cim. **A 24**, 369 (1974).
- [24] M. Vanderhaeghen, M. Guidal and J.-M. Laget, Nucl. Phys. A **627**, 645 (1997); Phys. Rev.

C 57, 1454 (1998).